Progress In Electromagnetics Research, Vol. 143, 315–330, 2013

INDUCTIVELYCOUPLED LOOP ANTENNA DESIGN FOR UHF RFID ON-BODY APPLICATIONS

Min-Chuan Tsai[1], Chien-Wen Chiu[1, *], Hwang-Cheng Wang[1], and Ter-Feng Wu[2]

[1]Department of Electronic Engineering, National Ilan University, Ilan 260, Taiwan

[2]Department of Electrical Engineering, National Ilan University, Ilan 260, Taiwan

Abstract—This paper presents a one-wavelength loop antenna fed by an inductively coupled loop for on-body applications. An equivalent circuit for the inductively coupled loop antenna is proposed to synthesize the antenna system with a microchip. The designed tag is printed on a PVC substrate and placed close to a four-layer stratified elliptical cylinder human model. The card-type tag measures $85.5 \times 54 \times 0.76\,\text{mm}^3$ and is suitable for use on a student ID card for a broad range of applications. The impedance bandwidth of the inductively coupled loop tag antenna is 60 MHz (880–940 MHz, 6.6%), which covers the operating UHF bands in U.S. and Taiwan. The measured reading distance ranges from 2.7 to 5.7 meters when placed at different positions on the chest of a human body in the open site.

1. INTRODUCTION

Radio frequency identification (RFID) has become a widespread technology in our daily life. RFID is employed for automatic identification and tracking of objects, and extensively used in supply chain management, health care, inventory management, animal tracking, and security, among others [1]. A passive (battery-less) RFID tag comprises an antenna and a microchip (application specific integrated circuit, ASIC) that has a transceiver embedded with a unique electronic product code (EPC) stored in EEPROM. Tags are always pasted on objects which need to be identified. For instance, an RFID tag printed on student ID card is used to record

Received 7 August 2013, Accepted 5 November 2013, Scheduled 8 November 2013

* Corresponding author: Chien-Wen Chiu (alexchiu@niu.edu.tw).

student information for various purposes on many university campuses. However, a UHF tag does not work well when it is placed close to a human body or held in hand. Because of the body-proximity effects, input impedance, radiation pattern, and realized gain of the tag antenna are influenced [2]. The influences are caused by absorption, diffraction, and scattering of electromagnetic waves due to the lossy and conducting human body. Thus, the performance of an RFID tag near a human body is seriously degraded. Therefore, the body-proximity effects must be investigated in advance when a tag is to be designed.

Researchers have carried out simulations of human-body effects on the tag antennas [3–6]. Marroco proposed a reference model of the human thorax to design an H-shape suspended patch tag antenna for on-body applications [3]. He used a four-layer cylinder to model skin/fat, bone, muscle, and average internal organs. In 2010, Occhiuzzi et al. reported a new antenna configuration combining folded conductors and tuning slots for wearable RFID sensor tag applications [4]. Rajagonpalan and Rahmat-Samii used two quarter-wavelength patches shorted to ground plane to design tag antenna for human monitoring applications [5]. In our laboratory, a card-type antenna with a long slot was proposed for tags put near a human body. However, the slot-type antenna is also susceptible to the influence of the human body [6]. Chen and Chuang found that loop antenna and its variants have comparatively better performance than dipole-type antennas with regard to the human body effects [7]. Some literature reported loop tag antenna design for UHF RFID applications. Im et al. used a folded dipole-loop with a capacitive load to design miniaturized tag antennas [8]. The proposed loop antenna has a compact structure with 80% size reduction. Wu et al. proposed a meander split ring like a gear to design a circular loop tag antenna with an inductively coupled feeding structure [9]. Liu et al. applied a capacitively-loaded inductively-coupled structure to feed a rectangular loop RFID tag antenna [10]. Their proposed antenna has an omnidirectional radiation pattern.

This paper proposes a loop antenna with an inductively coupled feed design for UHF RFID applications. An equivalent circuit model for the proposed feeding structure is derived to help synthesize the loop antenna. The proposed design is easy to implement since the design methodology is based on the equivalent circuit model and computational formulas. Necessary adaptation is then performed for the situation when the tag is put near a human body in practical applications. The thin loop antenna which has no ground plane makes it easy to apply on the student-ID card. Tags are also fabricated to

test the antenna performance and measure reading ranges.

In the remainder of the paper, Section 2 describes the characterization of the inductively coupled loop antenna. In Section 3, initial design methodology of the antenna in free space is introduced. In Section 4, the on-body design of the tag antenna pasted on a PVC card and put close to a stratified elliptical cylinder model of the human torso is described. This study measures the performance of the antenna by putting it on a stratified human model. Section 5 presents numerical results and discussions. The proposed antenna was fabricated and put on a real human body for test. The experiment shows that the achieved reading range is about 2.7 to 5.7 meters at different positions on the human body in the open site. Finally, Section 6 concludes the paper.

2. CHARACTERIZATION OF THE ANTENNA SYSTEM BY AN EQUIVALENT CIRCUIT MODEL

Figure 1 shows the configuration of the proposed tag antenna with a polyvinyl chloride (PVC) substrate whose relative dielectric constant (ε_r) is 2 and loss tangent ($\tan\delta$) is 0.0013. The dimensions of the PVC card measure 85.5 mm × 54 mm × 0.76 mm. The PVC card is also our student-ID card which is easy to obtain and fits in the pocket. However, polypropylene substrate (PP) or polyethylene (PET) will be a good alternative for RFID applications if mass production or cost is a main concern. The card-type tag printed on the student-ID card is put close to a simplified reference model of the human

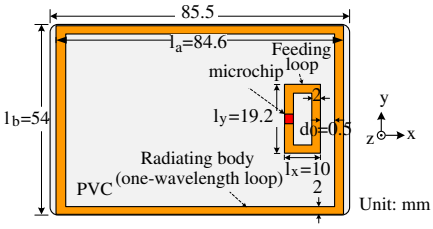

Figure 1. Geometry sizes of the loop antenna with an inductively coupled feed.

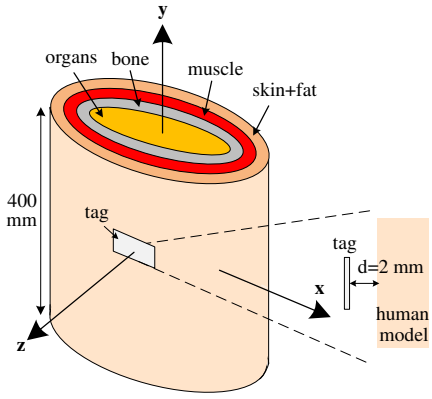

Figure 2. Elliptic cylinder human model.

Table 1. Physical and geometrical parameters of the human model at 915 MHz.

Layer	Relative Permittivity	Conductivity (σ in S/m)	Thin man (in mm^2)
Skin + Fat	14.42	0.24	335×168
Muscle	54.99	0.95	310×142
Bone	20.76	0.34	284×105
Organs	52	0.93	272×84

torso, as shown in Fig. 2. The approximate human model consists of a stratified elliptical cylinder with layer parameters shown in Table 1, which were obtained from the analysis of the anatomical maps in [3]. The tag is put at the center of the cylinder where the cylinder height is 400 mm. The proposed antenna consists of a feeding loop and a rectangular loop body. The feeding loop is located close to the main radiating body. Two terminals of the feeding loop are connected to a microchip. In this design, an *Impinj Monza*®4 tag chip [11] with an input impedance of $11 - j143\,\Omega$ at 915 MHz is utilized. The one-wavelength loop has better performance than the dipole-type antenna in on-body applications [7]. The near-zone field generated from the proposed loop antenna is dominantly magnetic. The tissue is less susceptible to the near magnetic field since the human tissue exhibits substantial dielectric loss [7]. Thus, the magnetic field is only slightly influenced by the human body when the antenna is put in the vicinity of the body.

The tag is initially designed in free space and then the designed antenna is miniaturized in Section 4 to fit on the reference model for on-body applications. In the free space, the proposed antenna can

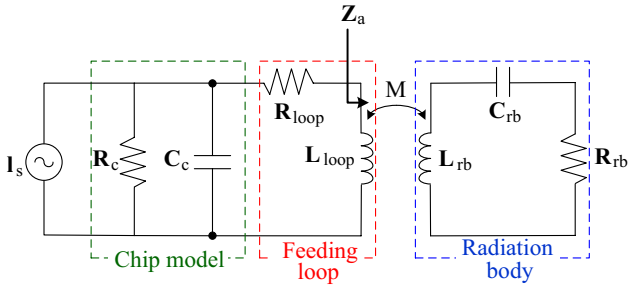

Figure 3. Equivalent circuit model of the proposed antenna.

be modelled as a lumped-element circuit, as shown in Fig. 3. The inductively coupled feeding model is based on Son's model which was proposed for an inductively coupled dipole tag antenna [12]. The radiating body is modelled as a series RLC resonant circuit: (R_{rb}, L_{rb}, C_{rb}). The feeding loop is modelled as a radiation resistance (R_{loop}) and a loop inductance (L_{loop}). The feeding loop is connected to a microchip which is modelled as a parallel RC circuit (R_c, C_c). Using the equivalent circuit model, the input impedance of the inductively coupled loop antenna is easily analyzed. Using a derivation similar to that in [12], the input impedance Z_a of the antenna system seen from the microchip terminals is given by

$$Z_a = Z_{feeding\ loop} + \frac{(2\pi f M)^2}{Z_{rb}}, \tag{1}$$

where $Z_{feeding\ loop}$ is the impedance of the feeding loop, and Z_{rb} represents the input impedance of the main radiating loop. M represents the mutual inductance between the feeding loop and the radiating loop. For operating frequency near the resonant frequency f_0, the input impedances of the radiating body and the inductively coupled feeding loop near resonance is calculated by

$$Z_{rb} = R_{rb,0} + jR_{rb,0}Q_{rb}\left(\frac{f}{f_0} - \frac{f_0}{f}\right), \tag{2}$$

$$Z_{feeding\ loop} = j2\pi f L_{loop}, \tag{3}$$

where $R_{rb,0}$ models the radiation resistance of the antenna body, Q_{rb} represents the quality factor of the radiating body, and L_{loop} is the self-inductance of the feeding loop. Substituting Equation (2) and Equation (3) into Equation (1), the real and imaginary parts of the input impedance Z_a are obtained, i.e.,

$$R_a = \frac{(2\pi f M)^2}{R_{rb,0}} \frac{1}{1 + \left[Q_{rb}\left(\frac{f}{f_0} - \frac{f_0}{f}\right)\right]^2}, \tag{4}$$

$$X_a = 2\pi f L_{loop} - \frac{(2\pi f M)^2}{R_{rb,0}} \frac{Q_{rb}\left(\frac{f}{f_0} - \frac{f_0}{f}\right)}{1 + \left[Q_{rb}\left(\frac{f}{f_0} - \frac{f_0}{f}\right)\right]^2}. \tag{5}$$

While the antenna system operates at the resonance condition ($f = f_0$), the real and imaginary parts of Z_a become

$$R_{a,0} = R_a(f = f_0) = \frac{(2\pi f_0 M)^2}{R_{rb,0}}, \tag{6}$$

$$X_a = X_a(f = f_0) = 2\pi f_0 L_{loop}. \tag{7}$$

Note that the antenna input reactance ($X_{a,0}$) depends only on the inductance (L_{loop}) of the feeding loop, and the input resistance ($R_{a,0}$) of the antenna is directly related to the mutual inductance (M) and the radiation resistance ($R_{rb,0}$). Using the equivalent circuit model, we can synthesize and design an inductively coupled loop antenna if the lumped-element values are evaluated in advance.

In order to approximately calculate the lumped-circuit parameters, each conductor segment is assumed to be a perfect conductor with uniform current and negligible loss. Fig. 4(a) shows the equivalent circuit of the feeding loop, which is comprised of a resistor and an inductor. The resistor R_{loop} represents the radiation resistance. Let the perimeter of the loop be represented as P. For a small loop ($P < \lambda_0/3$), the resistance is given as [13]

$$R_{loop} = 20\pi^2 \left(\frac{P}{\lambda_0}\right)^4. \tag{8}$$

Figure 4(b) shows the inductance computation model which consists of self and mutual parts. Referring to the Grover's formula [14], the self-inductance L in nano-henries of a straight filament of rectangular section with length l, width w, and thickness t in millimeters is given by

$$L = \frac{\mu_0}{2\pi} l \left[\ln\left(\frac{2l}{w+t}\right) + 0.50049 + \left(\frac{w+t}{3l}\right)\right] \; / \; 10^3 \,(\text{nH}). \tag{9}$$

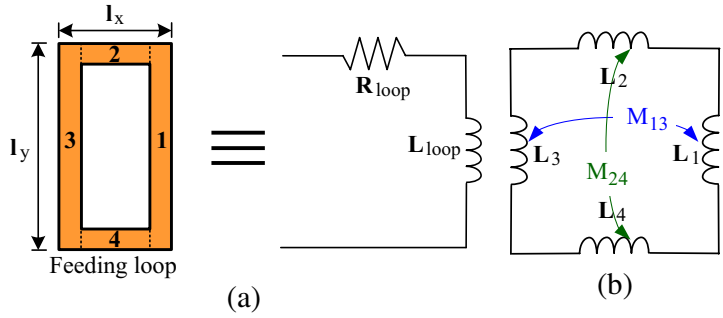

Figure 4. (a) Equivalent circuit of the feeding loop and (b) model of the inductor L_{loop}.

The mutual inductance M_p between two parallel filaments is given by

$$Q_p = \ln\left[\left(\frac{l}{d_{ab}} + \sqrt{1+\frac{l^2}{d_{ab}^2}}\right) - \sqrt{1+\frac{d_{ab}^2}{l^2}} + \frac{d_{ab}}{l}\right], \tag{10}$$
$$M_p = 2lQ_p,$$

where d_{ab} is the distance between the two filaments, l is the length of the filament as shown in Fig. 5, and Q_p is the inductance parameter [15]. Assume L_{gap} represents the line inductance of the gap between the feeding terminals. Then, the total inductance of the feeding loop with the gap is given by

$$\begin{aligned} L_{loop} &= (L_1 + L_2 + L_3 + L_4) - L_{gap} - 2(M_{13} + M_{24}) \\ &= 2(L_1 + L_2 - M_{13} - M_{24}) - L_{gap}. \end{aligned} \tag{11}$$

The main radiating body shown in Fig. 1 is a one-wavelength loop antenna which is simply modelled as an RLC series resonance circuit. The inductance of the radiating body combines with a series capacitor to resonate at its resonant frequency. According to [13], for an intermediate loop ($\lambda_0/3 \leq P < \pi\lambda_0$), the radiation resistance of the loop antenna can be modelled. The radiation resistance corresponds to the losses for the antenna during the transformation of the current into radiation wave. In general, total resistance contains radiation and loss resistance. Because the conductor of the proposed antenna is assumed to be lossless, $R_{rb,0}$ is equal to the total resistance and can be derived as

$$R_{rb,0} = \eta\pi\left(\frac{P}{\lambda_0}\right)^2 Q_{11}^{(1)}\left(\frac{P}{\lambda_0}\right), \tag{12}$$

where η is the intrinsic impedance of $120\pi\Omega$, P is the perimeter of the loop antenna, and $Q_{11}^{(1)}(\frac{P}{\lambda_0})$ is the integral that can be represented by

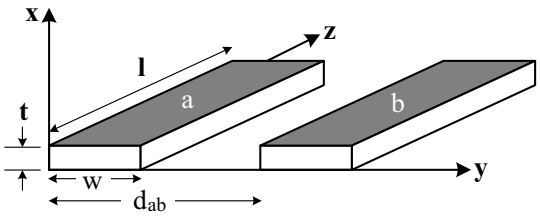

Figure 5. Two parallel strip lines for mutual inductance computation.

a series of Bessel functions as

$$Q_{11}^{(1)}\left(\frac{P}{\lambda_0}\right) = \frac{1}{\frac{P}{\lambda_0}} \sum\nolimits_{m=0}^{\infty} J_{2m+3}\left(2\frac{P}{\lambda_0}\right). \tag{13}$$

Therefore, substituting the perimeter P into Equation (13), $Q_{11}^{(1)}(\frac{P}{\lambda_0})$ can be computed by using MATLAB® and then substituted into Equation (12) to obtain $R_{rb,0}$. On the other hand, the inductance of the loop antenna is calculated by the formula in Grover's book [14]

$$L_{rb} = 0.4(l_a + l_b) \cdot \ln\left(\frac{2l_a \cdot l_b}{w(l_a + l_b)}\right). \tag{14}$$

After calculating the inductance values, we can get the capacitance and the quality factor from the relations in Equation (15)–(17) at resonance frequency. Thus,

$$\omega_0 = \frac{1}{\sqrt{LC}}, \tag{15}$$

$$C_{rb} = \frac{1}{(\omega_0)^2 L_{rb}}, \tag{16}$$

$$Q_{rb,0} = \frac{\omega_0 L_{rb}}{R_{rb}} = \frac{1}{\omega_0 R_{rb} C_{rb}}. \tag{17}$$

Consider the magnetic coupling between the inner feeding loop and the large loop. The parallel lines are approximated by two infinitely long wires ($l_b \gg l_y$) that carry currents of equal amplitudes and opposite directions. Thus, the mutual inductance between the feeding loop and line l_b as shown in Fig. 1 is given by [16]

$$M = \frac{\mu_0 l_y}{2\pi} \ln\left(\frac{(l_x + d_0)(l_a - d_0)}{d_0(l_a - l_x - d_0)}\right), \tag{18}$$

where μ_0 is the vacuum permeability and d_0 is the distance between the feeding loop and the main radiating loop.

3. INITIAL DESIGN IN FREE SPACE

In the previous section, the input impedance of the antenna in the free space was characterized and described. How to achieve conjugate match between the real and imaginary parts of the antenna impedance and those of the microchip is discussed in this section. In order to have maximum power transferring to the microchip, the input impedance of the designed antenna should be $Z_a = 11 + j143\,\Omega$ at 915 MHz. The resonant frequency f_0 is set to 915 MHz. The

desired inductive reactance of the antenna is 143 Ω at 915 MHz and thus the inductance (L_{loop}) of the feeding loop is about 24.87 nH by Equation (7). Using Equations (9)–(11), we designed a feeding loop structure with $l_x = 10.5$ mm and $l_y = 19$ mm. Using Equation (8), we can obtain the radiation resistance $R_{loop} = 0.21\,\Omega$. The main radiating body is a one-wavelength loop antenna. Consider the gap terminal influence and the parasitic effects due to the planar strip conductor. The one-wavelength loop antenna approximately resonates at $1.1\lambda_0$. We choose a rectangular loop antenna structure with $l_a = 108.5$ mm and $l_b = 77$ mm via HFSS EM simulation. The strip width of the main radiating loop is also set to 2 mm. The lumped-element parameters of the equivalent circuit model, R_{rb}, L_{rb}, C_{rb} and Q_{rb} are evaluated by using the formulas (14)–(17). The calculated inductance L_{rb} gives 282.52 nH by Equation (14) and the loop perimeter is about $1.1\lambda_0$. Using Equations (12) and (13), the radiation resistance $R_{rb,0}$ is about 249.61 Ω, which is computed by MATLAB. The calculated results by Equations (16) and (17) are $C_{rb,0} = 1.07 \times 10^{-13}$ F, and $Q_{rb,0} = 6.5$ at 915 MHz, respectively. Then, the evaluated mutual inductance (M) between the two loops is about 9.53 nH by Equation (18) if the distance d_0 between the two loops is set to 0.6 mm. Under the quasi-static approximations, we substitute the lumped-element values into Equations (4) and (5) to evaluate the input impedance. Fig. 6 shows the calculated input impedance of the inductively coupled loop antenna by calculation and a circuit simulator, Advanced Design System (ADS). It is unnecessary to tune and optimize the antenna system but it still operates well in the U.S. band. In order to validate these results, full-wave simulations by using HFSS EM simulator and measurements are performed. The calculated results are in good agreement with the measured data, confirming that the computed results by the equivalent circuit model are accurate and acceptable. Fig. 7 shows the return loss and power transmission coefficient of the inductively coupled loop antenna. The measured bandwidth ranges from 877 MHz to 958 MHz (8.8%). In comparison with the results obtained by full-wave simulation, the approximation error of measurements is small. In conclusion, the design by the equivalent circuit model is sufficiently accurate for real applications.

4. DESIGN ON A HUMAN MODEL

The initial design of the inductively coupled loop antenna as described in the previous section was directly printed on a PVC card and put close to the stratified elliptical cylinder human model, as depicted in Fig. 2. Due to the effects of the human model and the PVC card, the

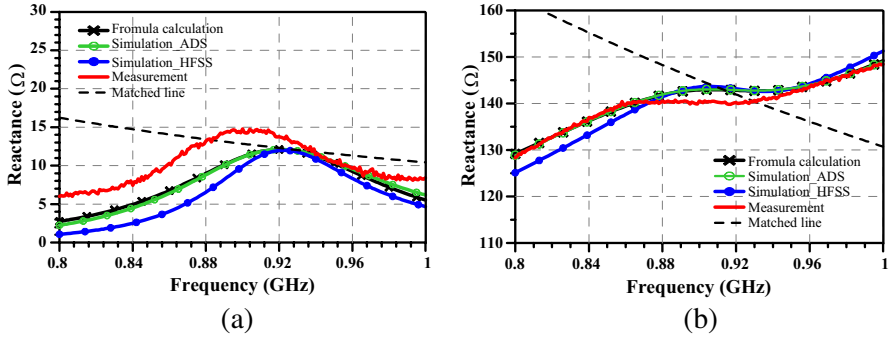

Figure 6. Input impedance of the inductively coupled loop antenna for initial design: (a) input resistance and (b) input reactance.

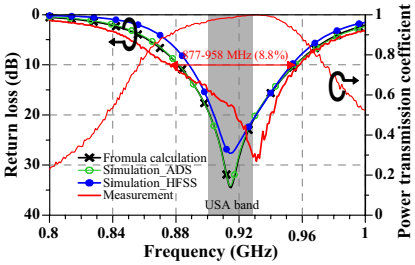

Figure 7. Return loss and power transmission coefficient of the inductively coupled loop antenna for initial design.

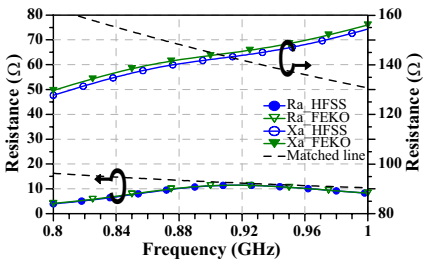

Figure 8. Input impedance of the inductively coupled loop tag antenna put on a human model.

effective dielectric constant of the antenna system will change. The loop antenna perimeter must be shrunk to fit on the human body. After some simulation test, it is decided that the first step is to change the total length of the main radiating body. The feeding loop and the coupling distance do not need to be modified. The perimeter of the loop is finally shrunk by about 25.3% according to our study. It satisfies our requirement at 915 MHz. Therefore, the perimeter of the loop is set to 277.2 mm and $l_a = 84.6$ mm, $l_b = 54$ mm are chosen in order to fit on a student ID card, as shown in Fig. 1. EM simulation reveals that we just need to fine-tune the feeding loop of the proposed antenna to complete the on-body antenna design process.

5. RESULTS AND DISCUSSIONS

Figure 8 shows the simulated impedance of the optimum antenna placed close to a human model by the HFSS. The measurements of the input impedance are not easy to accurately perform in our laboratory using a network analyser since we employed a simple cylinder model in the simulation instead of a real human body. Therefore, the simulated results are verified and compared with the results by the EMSS EM simulator, FEKO [17]. The comparison exhibits a good agreement between the two different results. It confirms the validity of our simulation using the HFSS EM simulator. Fig. 9 shows simulated return loss and power transmission coefficients compared with the results by FEKO. The transmission coefficient is near unity in the operating band as it reaches conjugate matching. The bandwidth ranges from 880 MHz to 940 MHz (6.45%), which covers the operating bands used in U.S. and Taiwan. Fig. 10 shows the realized gain and radiation efficiency of the proposed antenna by HFSS. Also shown in the figure for comparison are the simulated results by FEKO. The simulated results in this section are accurate and acceptable. The on-body gain is about -5 dBi at 915 MHz for the proposed design. The radiation efficiency of the loop antenna is about 10% in the operating band as it is put close to a human body. The study finds that increasing absorption due to the body effect will result in lower radiation efficiency when the antenna is put closer to the body. Combining the antenna with an artificial magnetic conductor (AMC) may improve the radiation efficiency since the AMC can insulate the antenna from the human body. However, the thickness of the substrate will be increased if wider operating bandwidth is concerned [18, 19].

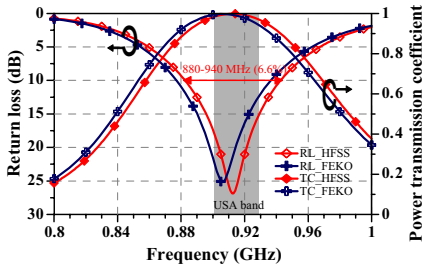

Figure 9. Return loss and power transmission coefficient of the inductively coupled loop tag antenna put on a human model.

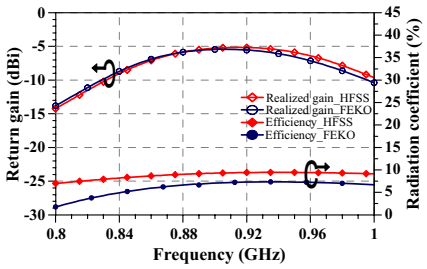

Figure 10. Realized gain and radiation efficiency of the inductively coupled loop tag antenna put on a human model.

The student-ID card will be bulky if the substrate thickness is over 1 mm. Thus, there is trade-off in the use of AMC to improve radiation efficiency.

The distance between the torso and the tag placed on the chest of a user is diverse in a real environment. The proximity effects on the tag are different at different distances d when the tag is placed near the human body. Fig. 11 shows the realized gain of the tag antenna as a function of distance d from the reference human model. In the operating band (902–928 MHz), there is little gain variation or degradation as the distance is changed. Fig. 12 shows simulated surface current distributions of the inductively coupled loop tag antenna at 915 MHz. The two nulls at the center of the upper and lower strips clearly indicate that the loop operates in one-wavelength mode. The

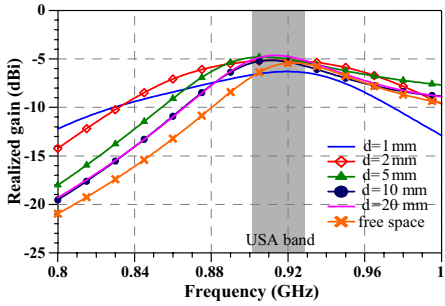

Figure 11. Realized gain of the inductively coupled loop tag antenna as function of distance d from reference human model.

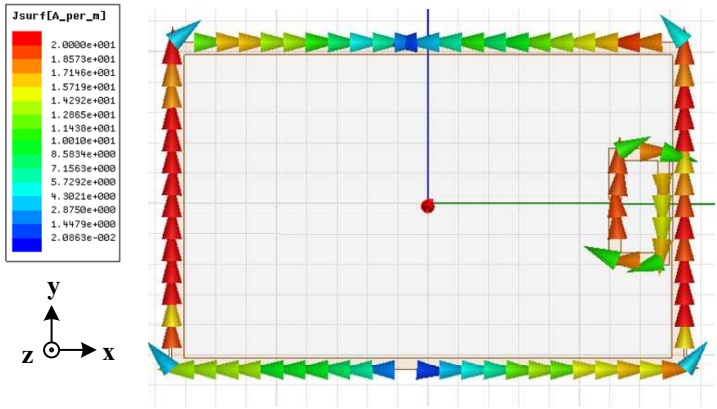

Figure 12. Simulated surface current distributions of the inductively coupled loop tag antenna at 915 MHz.

main radiation comes from the vertical current distribution. So, the loop antenna has a vertical polarization. Fig. 13 shows two-dimensional radiation patterns of the inductively coupled loop tag antenna attached on a human model at 915 MHz. Since some electromagnetic radiation was absorbed by the human model, the radiation energy is weak along the torso direction.

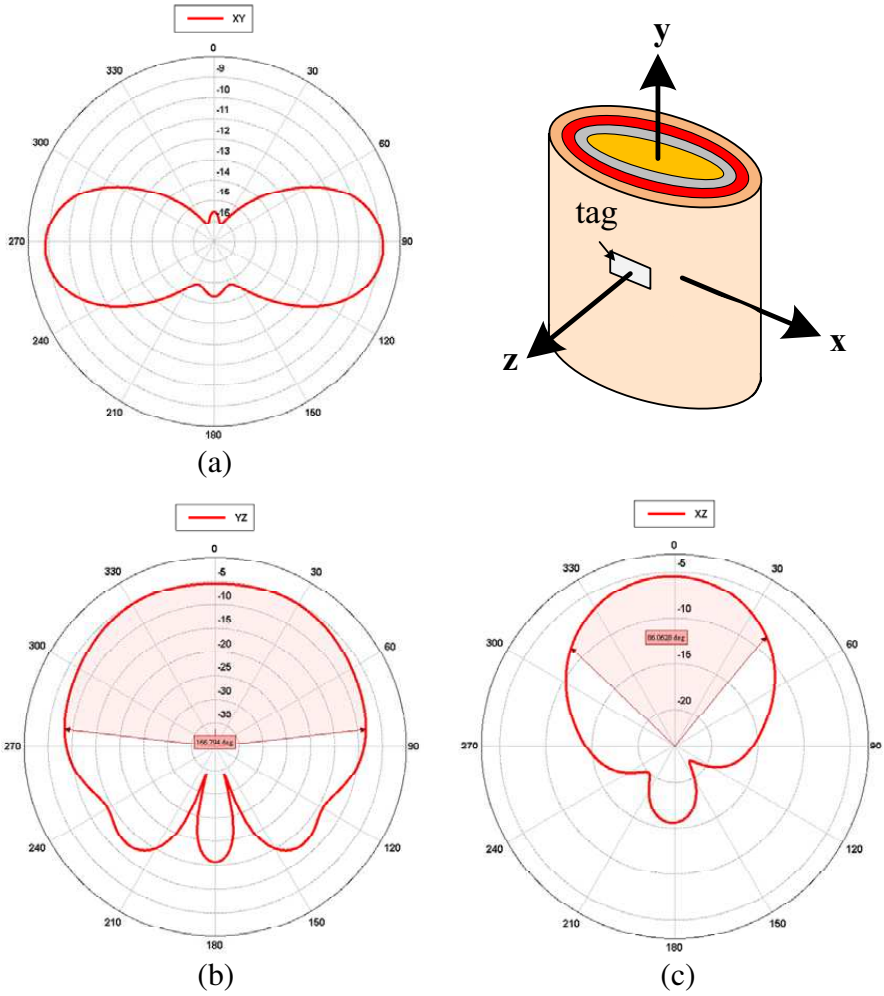

Figure 13. Two-dimensional radiation patterns of the inductively coupled loop tag antenna attached on a human model at 915 MHz. (a) XY-plane. (b) YZ-plane. (c) XZ-plane.

The forward reading range can be predicted using the Fri is free-space transmission formula [20]. The effective isotropic radiation power (EIRP) emitted by a reader is set to 4 W at 915 MHz. The minimum threshold power of the *Monza*®4 microchip is −17.4 dBm [11]. Circular polarization waves were sent by the reader. The polarization loss is approximately 3 dB since the loop antenna is a linear polarization antenna. The predicted reading range is about 4.8 m if the distance d between the tag and the reference human model is set to a fixed distance of 2 mm. In the experiment, the circularly polarized reader, *RU822*, has 4 W EIRP. The tag was oriented in the line-of-sight direction of the reader and pasted on the clothes near the chest of a human. Fig. 14 shows the tag positions when it was pasted on the chest of a human. The measured reading range is about 2.7 to 5.7 meters at different positions on a human body in the open site. Fig. 15 shows the prototype of the fabricated inductively coupled loop tag antenna. To conclude, the measured reading range is sufficient for practical applications in atypical university campus.

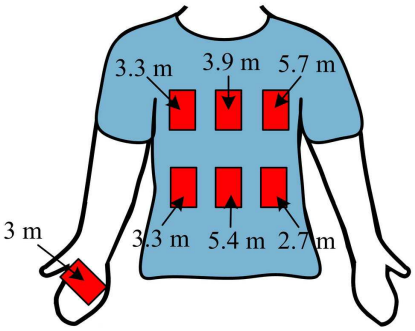

Figure 14. Different positions at the chest for reading range measurement.

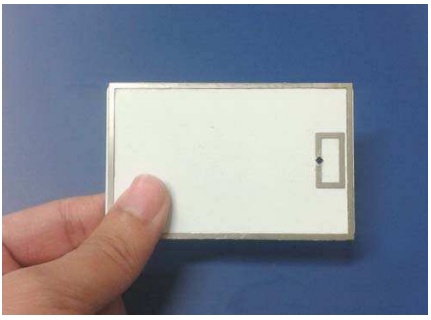

Figure 15. Photograph of the fabricated tag.

6. CONCLUSION

This paper presents a simple loop tag antenna printed on a PVC card for on-body applications. The equivalent circuit model was derived and applied to design the inductively coupled loop antenna. The performance of the antenna pasted on the chest of a reference model was simulated by HFSS and then verified by FEKO. The body-proximity effects have been considered and dealt with in the design stage. The proposed tag was fabricated to measure reading ranges.

It achieved a reading range of about 3–5 meters when it was pasted on a human body or held by hand. The proposed inductively-coupled loop tag antenna is suitable for use on student RFID cards for many practical applications.

ACKNOWLEDGMENT

The authors would like to thank the reviewers for their helpful comments which significantly improve the quality of the paper.

REFERENCES

1. Finkenzeller, K., *RFID Handbook: Fundamentals and Applications in Contactless Smart Cards and Identification*, 2nd Edition, Wiley and Sons, 2003.
2. Lin, M. H. and C. W. Chiu, "Human-body effects on the design of card-type UHF RFID tag antennas," *Proc. IEEE Symposium on Antennas and Propagation*, 521–524, 2011.
3. Marrocco, G., "RFID antennas for the UHF remote monitoring of human subjects," *IEEE Transactions on Antennas and Propagation*, Vol. 55, No. 6, 1862–1870, Jun. 2007.
4. Occhiuzzi, C., S. Cippitelli, and G. Marrocco, "Modeling, design and experimentation of wearable RFID sensor tag," *IEEE Transactions on Antennas and Propagation.* Vol. 58, No. 8, 2490–2498. Aug. 2010.
5. Rajagonpalan, H. and Y. Rahmat-Samii, "On-body RFID tag design for human monitoring applications," *Proc. IEEE Symposium on Antennas and Propagation*, 11–17, Jul. 2010.
6. Chiu, C. W., C. A. Ou, H. C. Wang, and Y. C. Chuang, "Slot antenna for UHF RFID tag close to the chest of a human body," *Microwave and Optical Technology Letters*, Vol. 53, No. 7, 1626–1631, Jul. 2013.
7. Chen, W. T. and H. R. Chuang, "Numerical computation of human interaction with arbitrarily oriented superquadric loop antennas in personal communications," *IEEE Transactions on Antennas and Propagation*, Vol. 46, No. 6, 821–828, Jun. 1998.
8. Im, Y. T., J. H. Kim, and W. S. Park, "Matching techniques for miniaturized UHF RFID loop antennas," *IEEE Antennas and Wireless Propagation Letters*, Vol. 9, 266–270, 2009.
9. Wu, J., J. X. Li, X. S. Cui, and L. H. Mao, "Circular loop antenna for UHF RFID tags with inductively coupled structure," *2011*

International Conference on Control, Automation and Systems Engineering (CASE), 1–4, Singapore, Jul. 30–31, 2011.

10. Liu, Q., Y. F. Yu, and Q. S. Huang, "Capacitively-loaded inductively-coupled fed loop antenna with an omnidirectional radiation pattern for UHF RFID tags," *PIERS Proceedings*, 195–197, Stockholm, Sweden, Aug. 12–15, 2013.
11. Monza® Datasheet, Available at http://www.impinj.com.
12. Son, H. W. and C. S. Pyo, "Design of RFID tag antenna using an inductively coupled feed," *Electronics Letters*, Vol. 41, No. 18, 994–996, Sep. 2005.
13. Balanis, C. A., *Antenna Theory: Analysis and Design*, 2nd Edition, Chap. 5, Wiley & Sons, 1997.
14. Grover, F. W., *Inductance Calculations: Working Formulas and Tables*, D. Van Nostrand, 1946.
15. Greenhouse, H. M., "Design of planar rectangular microelectric inductors," *IEEE Transactions on Part, Hybrid, and Package*, Vol. 10, No. 2, 101–109, Jun. 1974.
16. Zhang, J. and O. Breinbjerg, "Self-resonant electrically small loop antennas for hearing-aids application," *European Conference on Antennas and Propagation, EUCAP2010*, 1–5, Barcelona, Spain, Apr. 2010.
17. FEKO, EM Software & Systems-S.A. (Pty) Ltd. (EMSS), Available at http://www.feko.info.
18. Feresidis, A. P., S. Wang, and J. C. Vardaxoglou, "Artificial magnetic conductor surfaces and their application to low-profile high-gain planar antennas," *IEEE Transactions on Antennas and Propagation*, Vol. 53, No. 1, 209–215, Jan. 2005.
19. Sohn, J. R., K. Y. Kim, and H. S. Tae, "Comparative study on various artificial magnetic conductors for low-profile antenna," *Progress In Electromagnetics Research*, Vol. 61, 27–37, 2006.
20. Chen, Z. N., *Antennas for Portable Devices*, Wiley & Sons, 2007.